

Numerical Study on Effects of Obstacle Shape on Detonation Transition Mechanism

Ayu Ago¹, Tomotaka Niibo¹, Nobuyuki Tsuboi¹, A. Koichi Hayashi²

¹ Department of Mechanical and Control Engineering, Kyushu Institute of Technology, Kitakyushu, Fukuoka, Japan

² Department of Mechanical Engineering, Aoyama Gakuin University, Sagami-hara, Kanagawa, Japan

1 Introduction

Detonation is a combustion phenomenon with interacting shock waves and combustion waves, and propagates with supersonic in combustible premixed gas. As the detonation initiations, there is indirect initiation which includes DDT (Deflagration-to-Detonation Transition) and the DDT is initiated by a relatively small energy. Since the detonation can be initiated by a small energy, many experiments have been conducted from beginning of the research, and the distance from ignition to detonation (Detonation Induction Distance: DID) has been measured.

In 1940, Shchelkin et al. [1] showed that the detonation transition can be promoted when a coiled obstacle is installed along the channel inner wall. Urtiew and Oppenheim [2], which succeeded to measure the DDT process for the first time with laser Schlieren photographs, showed that the detonation is initiated by the local explosion occurring behind the leading shock wave generated by the turbulent flame in the channel. In 2000, Dorofeev et al. [3] introduced the characteristic geometric dimension L into the distance between obstacles installed at equal intervals in the channel. They showed that when the value (L/λ) obtained by dividing the length L by the detonation cell width λ exceeds 7, the detonation occurs. Although DDT has been investigated by many researchers, DDT has not been predicted theoretically because the DDT mechanisms change by physical conditions, for example, channel sizes and wall conditions. In recent years, numerical simulations on DDT are performed in small channel with repeated obstacle. Gamezo et al. [4] simulates DDT for using one-step Arrhenius kinetics model. They showed that a minimum space was necessary to ensure that the shock wave causes Mach reflection and initiates the detonation. It is found that the detonation transits at the triple point where the shock waves intersect.

This research intends to find out the mechanisms of the detonation transition in the channel with obstacles in order to understand the physical phenomena such as shock wave, turbulent flame, and local explosion caused by self-ignition by using the numerical analysis. In particular, two patterns of obstacle height are

used to investigate the detonation transition mechanisms. In this paper, the calculation domain size is based on the one-twentieth scale of the experimental device used by Dorofeev et al. [3], and two cases of obstacle heights are used in order to compare with their experiments.

2 Numerical Method and Simulation Conditions

In the channel with repeated obstacles, a stoichiometric premix gas of hydrogen/oxygen is filled and a small energy source near the left end of the channel is located.

The governing equations are the two-dimensional compressible Navier-Stokes equations including mass conservation of nine chemical species. For the convection terms, AUSMDV (Advection Upstream Splitting Method DV) scheme [5] is applied and its spatial accuracy is applied 2nd-order MUSCL (Monotonic Upstream-Centered Scheme for Conservation Laws) [6] including minmod limiter. The time integration method uses 3rd-order TVD Runge-Kutta (Total Variation Diminishing Runge-Kutta) method [7]. The source term is integrated by point implicit method. In the present simulation, the detailed chemical reaction model UT-JAXA [8] containing 9 species (H_2 , O_2 , N_2 , H , O , OH , HO_2 , H_2O_2 and H_2O) and 18 elementary reactions is adopted. Fick's law is used as mass diffusion. Thermal diffusion is ignored because it has small influence on combustion analysis. Wilke's coefficient equation is used for mixed average approach.

In this calculation, $5\mu\text{m}$ orthogonal grids are used. According to the ZND calculation, 12 grid points are contained in the half reaction length. Figure 1 shows the frame of the calculation grids used in this calculation. The calculation area is divided into 35 zones, and 17 obstacles are placed at regular intervals in the channel. As the number of zones is 35, the height is 2.25 mm and the width is 45.85 mm in the computational domain. The distance between obstacles is 1.75 mm, and the distance from the left end to the first obstacle is 3.35 mm. For the size of obstacles, the width is 0.75 mm, and the BR (blockage ratio: the value obtained by dividing the height of the obstacles by the channel width) has two patterns: 0.3 and 0.45. Furthermore, 11 grid points in the longitudinal direction are overlapped between two adjacent zones. Calculated physical values in each zones are interpolated to adjacent zone in order to calculate the divided zone as one area. Figure 2 and Table 1 show the number of grid points. The total number of grid points is about 3.7 million, and the calculation time is about 85 hours.

In the boundary conditions, the right boundary in the calculation area is set as an outflow condition, which is the non-reflection condition of Gamezo et al. [9]. The others are set as adiabatic non-slip wall conditions.

For initial condition, in the ambient area, pressure is 1 atm and temperature is 293 K, respectively. In the ignition area, initial pressure is 3 atm and initial temperature is 3000 K. The ignition area is a semicircle centered on the left end of the calculation region with a radius of 0.25 mm. Figure 2 shows the ignition area with an orange semicircle.



Fig. 1 Computational domain for DDT calculation with 17 obstacles (BR=0.3).

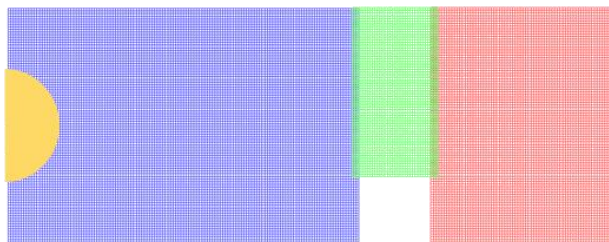


Fig. 2 Computational grid
(three on the left side of the whole).

Table 1 The number of grid points.

	BR: 0.3	BR: 0.45
Blue zone	451x671	451x671
Green zone	316x171	251x171
Red zone	451x351	451x351

3 Results and Discussions

3-1 Process of becoming a turbulent flame

Figure 3 shows the instantaneous flame front velocities for various obstacle heights. Since the propagation speed of the flame tip exceeds the CJ velocity, the deflagration transits to the detonation for BR=0.3 and 0.45. According to the experiments of Maeda et al. [10], compression waves preceding the flame diffract with the obstacles and create vortex rings. It is found that the flame was disturbed by being caught up in the vortices.

For BR = 0.3 and 0.45, in Fig. 4, it is observed that a vortex is generated near the boundary layer of the upper side of the obstacle after passing the preceding shock wave. The vortex created at the upper side of the obstacle is pulled by the main flow and comes off the wall surface. As the vortex involves the flame, it seems that the flame is disturbed as if the flame is swirling as shown in Fig. 4. In Fig. 3, it is shown that the flame is accelerated by repeating the narrowing and spreading of the flow path by the obstacles. The surface area of the flame is increased due to the disturbance of the flame caused by obstacles, and the combustion is promoted. Therefore, several compression waves are generated, and the strong shock wave is created in front of the flame.

3-2 Effects of obstacle height

In Fig. 3, it is shown that for BR = 0.3 and 0.45, the times of transition from deflagration to detonation are different. It is earlier about 10 mm ahead of the ignition position for BR = 0.3. In addition, the number of local explosions that occurred before transition to detonation is different, the local explosion occurred twice for BR = 0.3 and five times for BR = 0.45.

First, the detonation transition for BR = 0.3 is described. For BR = 0.3, Figure 5 shows a local explosion near the lower corner of the 6th obstacles. However, it is immediately swallowed by the burned gas and the flame does not transit to the detonation. In Fig. 5 the reflected shock waves (RS) and the shock waves caused by the local explosion (SWD) interact with the flame near the 8th obstacle and the flame transits to detonation. Secondly, for BR = 0.45 in Fig. 6, a local explosion, which triggers the detonation transition before the 12th obstacle, is observed. The reason of the local explosion would be the interaction between the shock waves reflected by the obstacle and the lower wall of the channel. However, the local explosion is surrounded by the burned gas and it is swallowed by the burned gas. The shock wave which is created by the local explosion reaches the upper wall of the channel and reflects. This reflected shock wave overlaps the incident shock wave to form a Mach stem and to become the detonation wave. The detonation transition similar to the above phenomena was also shown by the numerical study by Goodwin et al. [11]. We compare with BR = 0.3 and 0.45, although the flame propagation velocity is almost the same from the left channel end to about 20 mm, the times of transition to detonation are different. Considering this reason, it was found that there are four local explosions that do not transit to detonation. Since two-dimensional numerical analysis does not consider the unburned gas remaining in the depth direction, the higher the obstacle, the smaller area of the unburned gas that remains in front. Therefore, even if a local explosion occurs, transition to detonation is failed because it is swallowed by the mainstream flame. Also, in Fig. 7, for BR = 0.45, the shape of the flame just before transitioning to detonation is similar to a type of flame called tulip flame. There are little unburned gas in the area between the flame and the upper wall, and the local explosion caused by the reflection shock wave is less likely to occur. Therefore, it is considered that the transition was delayed, compared to the case of BR = 0.3.

3-3 Comparison with experiment results

Dorofeev et al. [3] reported that detonation is observed when the ratio of characteristic geometrical size L to the detonation cell width λ exceeds 7. In Fig. 8, L represents the following Eq. (1). Table 2 shows the relation between the detonation transition and L/λ . The detonation cell width is 1.4 mm in this condition.

Although $L/\lambda < 7$ for BR = 0.3 and 0.45, the deflagration transits to the detonation. The present results do not agree with their experimental results. The present calculation domain is 1/20 scale of their experiment and the present calculation is two-dimensional. Maeda et al. [10] reported that three-dimensional effects are important on the detonation transition because the detonation transition starts near the side wall. Therefore dimensional effects are important on DDT in the present conditions.

In addition, Dorofeev et al. [3], explained that $L/\lambda < 7$ holds even if the scale of the channel is changed. However, as the channel width is narrow as in this case, the influence of viscosity strongly appears. That is why an exact comparison of the results with the experiment may be difficult. It would be interesting to investigate the scale effect as future works.

$$L = \frac{S}{1 - d/H} \quad (1)$$

4 Conclusions

The numerical simulations on DDT in the two-dimensional channel with the repeated obstacles are performed for various BR values. For BR = 0.3 and 0.45, the deflagration transits to the detonation. The flames were becoming turbulent by involving the vortex generated by the boundary layer on the upper surface of the obstacles. When the detonation transition occurs, the flame is largely disturbed. Then the flame is accelerated by the repeated local explosions, the compression and expansion in the flow path, and strengthened shock wave. Also, even if local explosions occur, the detonation transition is failed, and for BR = 0.45, the detonation transition is delayed as compared with BR = 0.3 because of high obstacles. Comparing with the experimental results, it is found that the effects of the geometry scaling, the ignition source, the wall condition, and three-dimensional depth should be estimated.

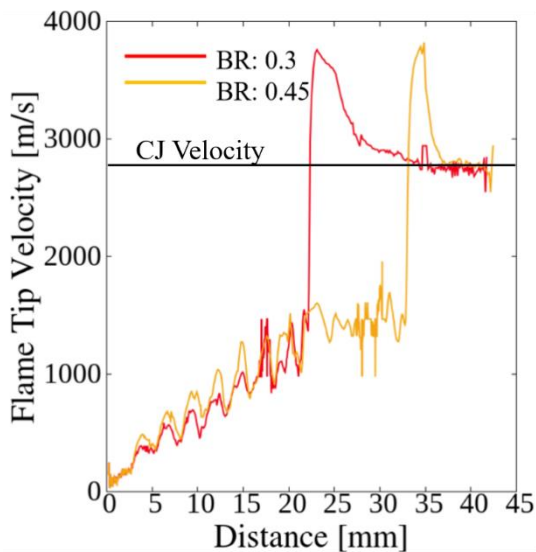


Fig.3 Propagation velocities of flame front. Red line shows result for BR = 0.3 and orange line for BR = 0.45.

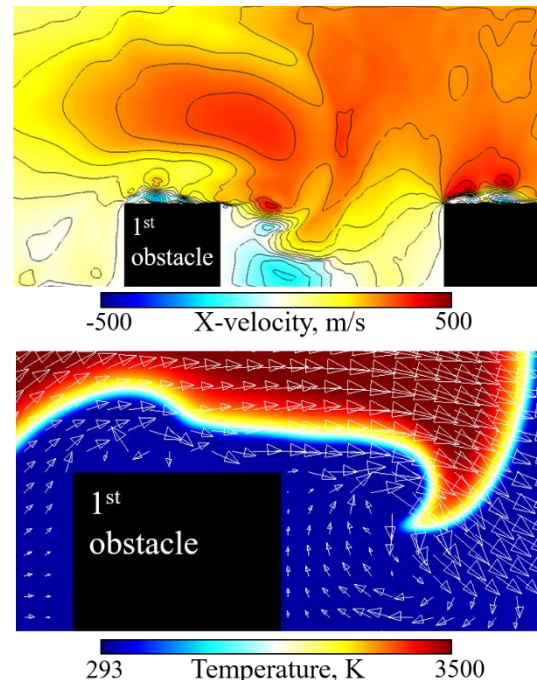


Fig. 4 The upper figure shows the flow velocity (in the horizontal direction) distribution and the lower figure shows the temperature distribution for BR = 0.3.

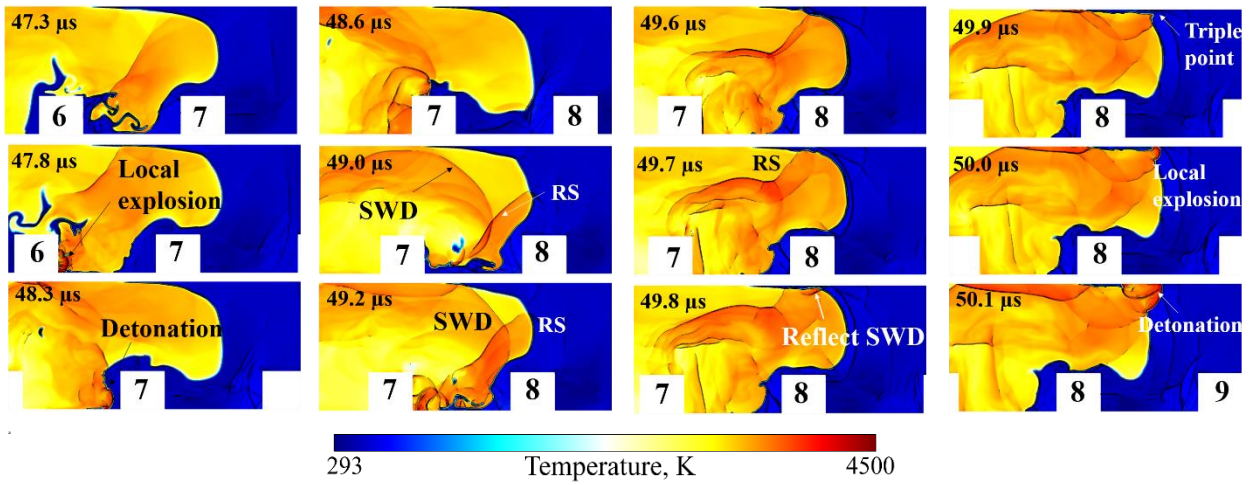


Fig. 5 Temperature distributions on schlieren contours for BR = 0.3. Close up to 6th and 9th obstacle. Time increases downwards on left column and sequence continues on right column.

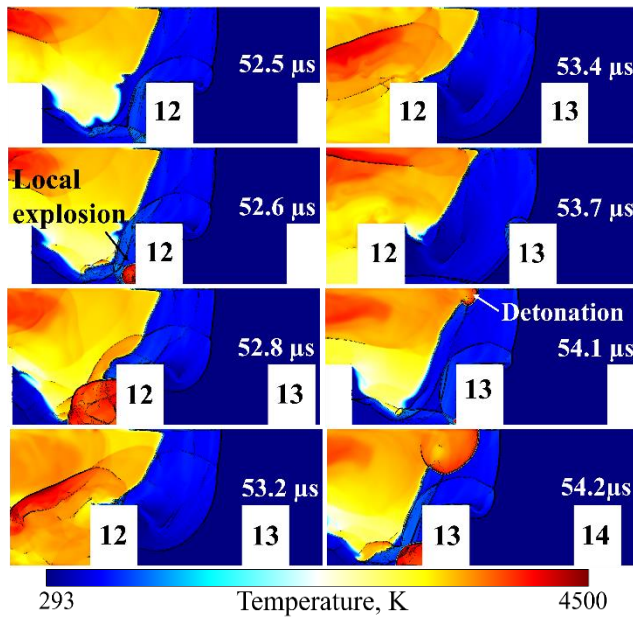


Fig. 6 Temperature distributions on Schlieren contours for BR = 0.45. Close up to 12th and 13th obstacle.

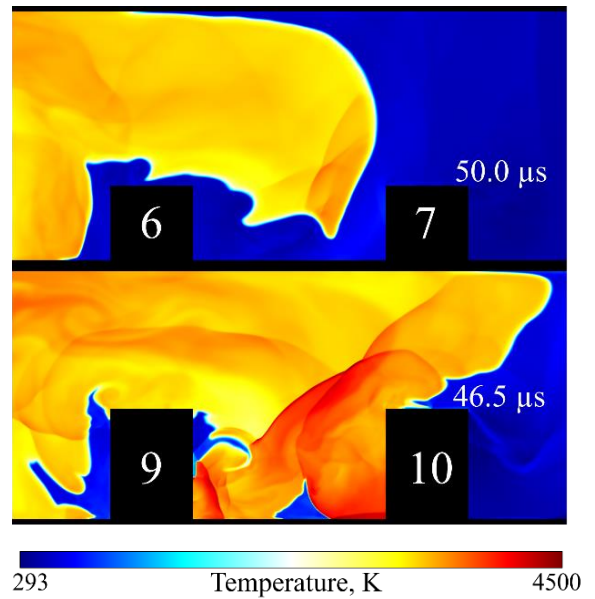


Fig. 7 Temperature distributions just before transition to detonation. The upper figure shows BR = 0.3 and the lower shows BR = 0.45.

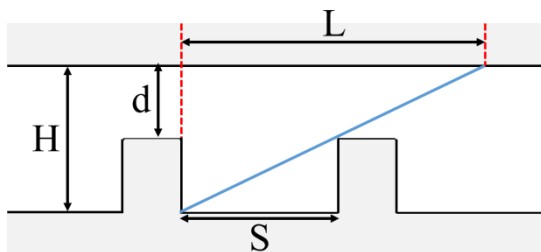


Fig. 8 Schematic figure of characteristic size L .

Table 2 Relationship between L/λ and transition to detonation.

	BR: 0.3	BR: 0.45
L/λ	4.17	2.81
transit to detonation	detonation	detonation

Acknowledgments

The authors would like thank Dr. Morii for his advice in the present simulations. The numerical simulations were carried out in the Super Computing system in Osaka University. This study is also supported by Japan Nuclear Fuel Ltd.

References

- [1] Shchelkin K. L., (1940). Influence of Wall Roughness on Initiation and Propagation of Detonation in Gases. *Zh. Eksp. Teor. Fiz.* 10: 823-827
- [2] Urtiew P. A. and Oppenheim A. K., (1966). Experimental observation of the transition to detonation in an explosive gas. *Proc. Roy. Soc. London Series. A* 295: 13-28
- [3] Dorofeev S. B., Sidorov V. P., Kuznetsov M. S., Matsukov I.D. and Alekseev V.I., (2000). Effect of scale on the onset of detonations. *Shock Waves.* 10: 137-149
- [4] Gamezo V. N., Ogawa T. and Oran E. S., (2008). Flame acceleration and DDT in channels with obstacles: Effect of obstacle spacing. *Combustion and Flame.* 155: 302-315
- [5] Wada Y. and Liou M. S., (1997). An Accurate and Robust Flux Splitting Scheme for Shock and Contact discontinuities *SIAM Journal on Scientific Computing.* 18(3): 633-657
- [6] Van Leer B., (1979). Towards the ultimate conservative difference scheme. V. A second-order sequel to Godunov's method. *Journal of Computational Physics.* 32(1): 101-136
- [7] Gottlieb S. and Shu C. W., (1998). Total variation diminishing Runge-Kutta schemes. *MATHEMATICS OF COMPUTATION.* 67: 73-85
- [8] Shimizu K., Hibi A., Koshi M., Morii Y. and Tsuboi N., (2011). Updated kinetic mechanism for high pressure hydrogen combustion. *JOURNAL OF PROPULSION AND POWER.* 27(2): 383-395
- [9] Gamezo V. N., Desbordes D. and Oran E. S., (1999). Two-dimensional reactive flow dynamics in cellular detonation waves. *Shock Waves.* 9(1): 11-17
- [10] Maeda S., Minami S., Okamoto D. and Obara T., (2016). Detonation transition process in a channel equipped with the repeated obstacles (Effect of obstacle height and spacing on the DDT process), *Transactions of the JSME (in Japanese).* 82(834)
- [11] Goodwin G. B., Houim R. W. and Oran E. S., (2016) Effect of decreasing blockage ratio on DDT in small channels with obstacles, *Combustion and Flame.* 173: 16-26